Steam reforming of methanol over copper loaded anodized aluminum oxide (AAO) prepared through electrodeposition

CrossMark

E. Linga Reddy [a, *], J. Karuppiah [b], Hyun Chan Lee [a], Dong Hyun Kim [a]

[a] Department of Chemical Engineering, Kyungpook National University, Daegu 702-701, Republic of Korea
[b] Department of Chemical and Biological Engineering, Jeju National University, Jeju 690-756, Republic of Korea

HIGHLIGHTS

- A porous structured Al_2O_3/Al supported Cu catalyst was developed for SRM reaction.
- SRM conversion and CO_2 selectivity are increased with Cu content.
- AAO surface area was enlarged with hot water treatment process.
- The AAO-HWT supported catalysts series has shown higher SRM activity.

GRAPHICAL ABSTRACT
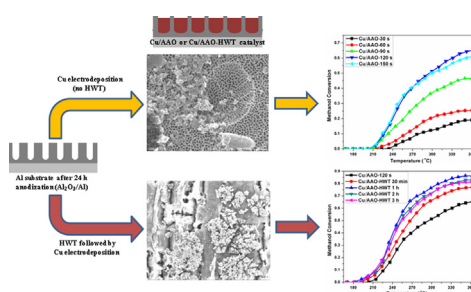
ARTICLE INFO

ABSTRACT

In order to study the steam reforming of methanol (SRM) to produce hydrogen for fuel cells, porous γ-alumina support is developed on Al substrate using anodic oxidation process and copper catalyst particles are deposited homogeneously over anodic aluminum oxide (AAO) surface by electrodeposition method. We investigated the effect of electrodeposition time and hot water treatment (HWT) on the activity of catalysts for SRM reaction in the temperature range between 160 and 360 °C. The experimental results indicate that the SRM activity, CO_2 and dimethyl ether (DME) selectivity's over Cu catalysts increased as the electrodeposition time increased from 30 to 120 s, further increment in deposition time of Cu have no significant effect on it. The rates of SRM conversion are found to be higher for the catalysts made from the supports obtained after HWT, which may be due to the enhancement in the surface area of AAO support. It is found that the SRM activity and CO_2 selectivity strongly depended upon the free exposed copper sites available for methanol adsorption and reaction, and DME in products is mainly observed in the reaction temperature range between 300 and 350 °C and it is higher for the catalysts with low Cu content.
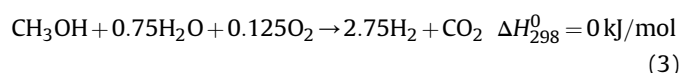
1. Introduction

Hydrogen is considered as a present and future energy resource especially for fuel cells to produce electricity [1]. It can be generated on-board using liquid hydrogen carrier such as methanol [2,3], ethanol [4], dimethyl ether [5], etc. Among the sources methanol has several advantages for hydrogen production when compared to the other liquid organics. Hydrogen can be easily produced from methanol by following three processes: (1) partial oxidation of methanol (POM), (2) steam reforming of methanol (SRM) and (3) oxidative steam reforming of methanol (OSRM)

$$CH_3OH + \frac{1}{2}O_2 \rightarrow 2H_2 + CO_2 \quad \Delta H^0_{298} = -192.3 \text{ kJ/mol} \quad (1)$$
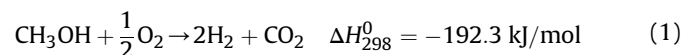
* Corresponding author. Tel.: +82 53 950 4786; fax: +82 53 950 6615.
  E-mail address: elreddy@knu.ac.kr (E. Linga Reddy).

$$CH_3OH + H_2O \rightarrow 3H_2 + CO_2 \quad \Delta H^0_{298} = 49.4 \text{ kJ/mol} \tag{2}$$

$$CH_3OH + 0.75H_2O + 0.125O_2 \rightarrow 2.75H_2 + CO_2 \quad \Delta H^0_{298} = 0 \text{ kJ/mol} \tag{3}$$
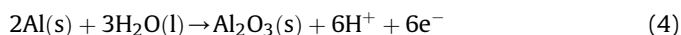
Among the methods, SRM can produce H_2/CO_2 in the molar ratio of 3/1. Mainly, copper-based catalysts are used for the above reactions due to their high activity and excellent selectivity for CO_2, and the reaction occurs at low temperatures in the range between 200 and 350 °C [6–9] and the products are mainly hydrogen and carbon dioxide with a small amount of CO, usually less than 1%, as a by-product [10,11].

Present technology for methanol reforming uses packed-bed type catalytic reactors that deteriorate from a number of inherent problems such as precipitous temperature gradients caused by poor thermal conductivity of the catalyst bed as well as large pressure loss through the bed. The temperature gradient in the reactor can cause a hot spot which results in poor performance due to catalyst deactivation by sintering and generation of a large amount of CO [12–14]. To overcome this, a metal monolith type reactor has been suggested as a promising solution as these reactors allow rapid heat transfer along the axial direction of the reactor by conduction through the wall, thereby reducing the temperature gradient. The metal monolith type support is usually made of a high thermal conductivity as well as high mechanical durability metal such as aluminum [14] and has a large metal area, on which a catalyst layer can be grown or coated. This type of reactor is differentiated by a low pressure drop and easy to scale up or scale down.

To prepare a high conductivity metal monolith type reforming catalyst support, it should be formed on the metal surface. One of the effective ways of forming a layer of catalyst support on the metal surface is anodic oxidation, an electrochemical process that forms various metal oxides. It is well known that alumina is an effective catalyst support, when methanol is reformed. Anodic oxidation of aluminum occurs within an electrolyte bath when aluminum is connected to an electric-current source as an anodic electrode, while graphite is used as a cathode [15,16]. The anodic electrode surface is oxidized based on the following reaction formulas ((4)–(6))
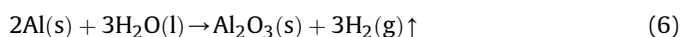
Anode:

$$2Al(s) + 3H_2O(l) \rightarrow Al_2O_3(s) + 6H^+ + 6e^- \tag{4}$$

Cathode:

$$6H^+ + 6e^- \rightarrow 3H_2(g)\uparrow \tag{5}$$

Overall:

$$2Al(s) + 3H_2O(l) \rightarrow Al_2O_3(s) + 3H_2(g)\uparrow \tag{6}$$

The development of a preparation method that loads catalytic components onto the support is very important task. The point of preparation method is to achieve the deposition of catalytic component with a high performance and a strong adhesion onto the substrate. The impregnation method [17], wash coat method [18–20], immersion method [21–24] and the electroless plating method [25–28] have been reported so far as the preparing method of the structured catalysts. In each method, many attempts that enlarge a specific surface area and a TOF of active site for the catalyst were performed respectively. However, for corresponding to the variety of the constructed reaction field and of the targeted chemical raw material, it is necessary to develop another preparation method that has wider applicability in the catalyst preparation. From such viewpoint, we have mainly investigated about the electrodeposition technique as a novel method for preparing the structured catalyst for methanol steam reforming reaction.

In the present study, we have developed the porous anodic aluminum oxide plates (Al_2O_3/Al) as catalytic support and a new preparation method based on the electrodeposition was investigated for the preparation of structured Cu catalyst supported on AAO and the activity of prepared catalyst was studied for the methanol reforming reaction in a tubular reactor. Especially, the electrodeposited Cu/AAO structured catalyst for the methanol steam reforming reaction has been targeted.
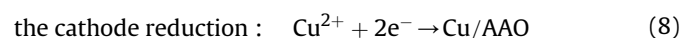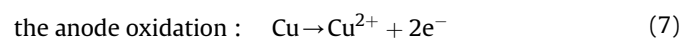
2. Experimental

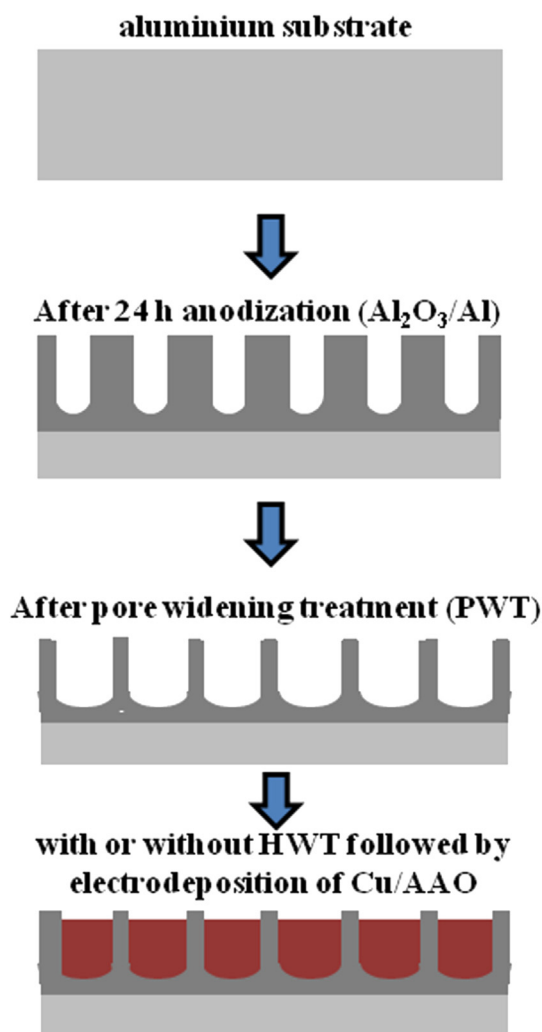### 2.1. Catalyst support preparation

A high purity (99.99%) aluminum sheet (10 cm × 12 cm, 1 mm thick) was first degreased with acetone for 30 min followed by 10 min of ultrasonic cleaning in distilled water and then annealed at 400 °C in air for 3 h to remove mechanical stress and then was cleaned with acetone followed by distilled water. Further the foil was anodized in a 0.3 M oxalic acid at 40 V (direct current (DC)) for 24 h at 10 °C to form a porous γ-alumina layer, whereas graphite plate was used as cathode. After the formation of porous γ-alumina layer, pore widening treatment (PWT) was carried out by dipping the plate in the same oxalic acid solution used for anodization at 30 °C for 4 h and is schematically drawn in Fig. 1. After completion of PWT, plate was washed in deionized water at room temperature for enough time to remove residual oxalic acid. Further, it was subjected to hot water treatment (HWT) in deionized water at 95 °C for 30 min, 1 h, 2 h, 3 h and these samples were indicated as AAO-HWT-30 min, AAO-HWT-1 h, AAO-HWT-2 h and AAO-HWT-3 h, respectively. Finally, the AAO samples with a high surface area were obtained by calcination in air at 450 °C for 4 h. The prepared AAO supports were cut into two pieces of 5 × 12 cm.

2.2. Electrodeposition of Cu over AAO supports

Electroplating is the process of deposition of a metallic coating onto an object (AAO in the present study) by putting a negative charge onto the object and immersing it into a solution that contains a salt of the metal to be deposited [29]. In this work, the formation of copper plating on AAO surfaces can be represented by the following Equations (7) and (8):

$$\text{the anode oxidation :} \quad Cu \rightarrow Cu^{2+} + 2e^- \tag{7}$$

$$\text{the cathode reduction :} \quad Cu^{2+} + 2e^- \rightarrow Cu/AAO \tag{8}$$

The experimental apparatus for the Cu electrodeposition over porous AAO template was shown in Fig. 2. A gold sputtered AAO template was used as cathode; whereas a copper plate (99.99% pure) and Ag/AgCl electrode were used as an anode and a reference electrode. The aqueous solution containing $CuSO_4$ (120 g L^{-1}) and H_3BO_3 (45 g L^{-1}) was used as electrolyte solution for electrodeposition of Cu metal particles. Electrolyte solution was magnetically stirred during experiments to ensure proper mixing of Cu ions and to prevent depletion of ions near the electrode surface. The Cu metal particles were electrochemically deposited by using this template synthesis technique [30] (is schematically drawn in Fig. 1) at room temperature and at a constant cathodic current density of 70 A m^{-2}. The AAO samples prepared with different plating time i.e., 30, 60, 90, 120 and 150 s indicates as Cu/AAO-30 s, Cu/AAO-60 s, Cu/AAO-90 s, Cu/AAO-120 s and Cu/AAO-150 s, respectively. In a similar way HWT treated samples also underwent for Cu electrodeposition at constant time (120 s) and the resulted catalyst

aluminium substrate

After 24 h anodization (Al$_2$O$_3$/Al)

After pore widening treatment (PWT)

with or without HWT followed by electrodeposition of Cu/AAO

Fig. 1. Schematic representation of the anodic aluminum oxide (AAO) template growth and the steps involved in the preparation of Cu/AAO catalyst.

samples were denoted as Cu/AAO-HWT 30 min, Cu/AAO-HWT 1 h, Cu/AAO-HWT 2 h and Cu/AAO-HWT 3 h, respectively. After deposition, the obtained samples were washed several times with distilled water and dried in an oven at 80 °C for 12 h.

2.3. Catalyst characterization

The BET specific surface area of the obtained AAO samples was determined using the nitrogen adsorption method (Micromeritics ASAP 2020), where outgas operation was set at 300 °C for 2 h. The XRD patterns of the catalysts were collected on a Rigaku Powder Diffractometer (D/Max-2500) using Cu-Kα radiation in the 2θ range of 20—80°. Metal loading in the SRM catalyst was determined using ICP-OES system (Optima 7300DV, Perkin Elmer) with a dual view (axial and radial) at the 40 MHz frequency in the wavelength range of 165—783 nm. The surface morphology of AAO was measured on a FE-SEM (JEOL JSM-6701F) machine at an accelerating voltage of 10 kV. The copper loading in the catalyst samples was confirmed by EDAX (HITACHI S-4800) attached to FE-SEM. Prior to the analysis, the sample surface was coated with Pt to enhance the conductivity of the sample. The copper surface area was measured via N_2O dissociation over the catalyst samples [31]. A 150 mg sample was first reduced at 300 °C for 2 h under a 10% H_2/He mixture that flowed at 50 mL min^{-1}. Then the sample was cooled to 80 °C under He flow, and a 100 μL N_2O pulse was injected in a series of 10 min intervals using He as the carrier gas (25 mL min^{-1}). The N_2 and N_2O in the effluent were separated in a Porapak N column (1.8 m and 1/8 inch) at room temperature and analyzed with a TCD detector.

2.4. Steam reforming of methanol experiment

SRM is carried out in a fixed bed reactor over a temperature range of 160—360 °C at atmospheric pressure. The catalyst was cut into pieces (2—3 mm^2 size) and packed into a 1/4 inch quartz tube reactor. The temperature of the reactor was increased at a rate of 0.7 °C min^{-1}. A methanol and a water saturator were used separately to vaporize the liquid feed. N_2 was used as a carrier gas to carry the vapors from each saturator and flow rate of N_2 was controlled by using mass flow controllers. A water circulating baths were used to control the temperature of each saturator. The feed composition to the reactor was 10% CH_3OH, 15% H_2O and balance N_2 with a total flow rate of 100 mL min^{-1}. The effluent composition was analyzed online by a gas chromatograph equipped with a
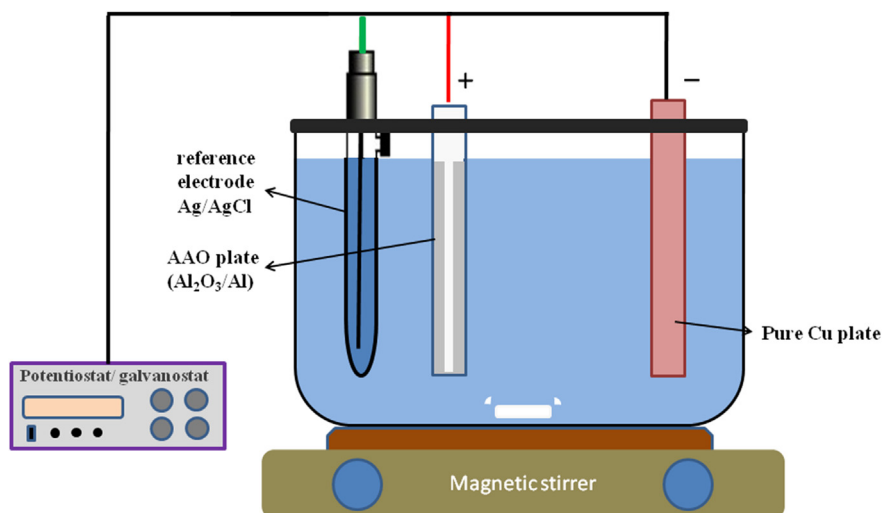
Fig. 2. Experimental apparatus for electrodeposition of copper metal particles over AAO.

thermal conductivity detector (TCD), Porapak Q column was used to separate CO_2, CH_3OH, DME and H_2O at the reactor outlet. The performance of the catalyst was analyzed in terms of methanol conversion. The methanol conversion was defined as the mole ratio of gaseous carbon compounds (CO, CO_2 and DME) in the product stream to the feed methanol.

3. Results and discussion

3.1. Characterization

The amount of copper loading, BET surface area and copper metal surface area of the catalyst and support itself are shown in Table 1. The BET surface area of the HWT treated AAO support (47.21 $m^2 g^{-1}$ for AAO-HWT 1 h) was higher than that of the untreated AAO (28.8 $m^2 g^{-1}$). This is because the HWT treatment process consequently opened the pores of AAO and enlarged the surface area. Also at the HWT conditions only the top layer of AAO film is hydrated and rest of the film retains its porous structure. However, there was a large improvement in the surface area was observed, for example 47.21 $m^2 g^{-1}$ was obtained for AAO-HWT 1 h support. At higher HWT treatment time (more than 1 h) does not much influenced on surface area enhancement. Further, the surface area gradually decreased with copper loading on to the pores of AAO. From N_2O dissociation studies, the copper metal surface areas of the AAO supported catalysts are 0.846, 1.54, 1.89, 2.81 and 2.94 $m^2 g^{-1}$ has been obtained for Cu/AAO-30 s, Cu/AAO-60 s, Cu/AAO-90 s, Cu/AAO-120 s and Cu/AAO-150 s catalysts, respectively. For the AAO-HWT supported catalysts, Cu metal surface areas are 3.29, 3.82, 3.65, and 3.2 $m^2 g^{-1}$ for Cu/AAO-HWT 30 min, Cu/AAO-HWT 1 h, Cu/AAO-HWT 2 h, and Cu/AAO-HWT 3 h catalysts, respectively. As seen from Table 1, copper metal surface area gradually increases with deposition time up to 120 s after that the increment is very low from120 to 150 s deposition, and in the case of HWT treated catalysts also copper metal surface area is higher than untreated AAO catalysts. Up to a certain loading time, the copper deposited on the pores of AAO homogeneously, and after maximum distribution of copper metal particles into the micropores, further loading resulted in clusters of copper agglomerates and reduced the further copper deposition.

From ICP-OES analysis a Cu wt% of 1.42, 1.98, 2.86, 4.152 and 4.28 has been observed for Cu/AAO-30 s, Cu/AAO-60 s, Cu/AAO-90 s, Cu/AAO-120 s, and Cu/AAO-150 s catalysts, respectively. For the Cu/AAO-HWT catalysts, a Cu wt% of 4.49, 5.218, 5.24 and 5.18 for Cu/AAO-HWT 30 min, Cu/AAO-HWT 1 h, Cu/AAO-HWT 2 h, and Cu/AAO-HWT 3 h, respectively was observed. The higher Cu content
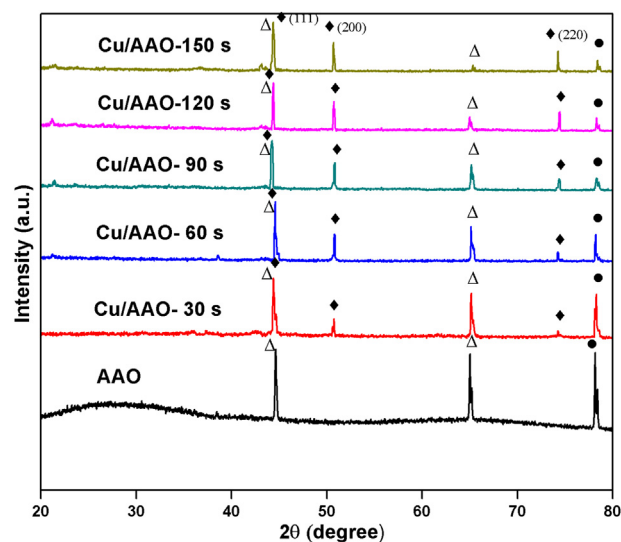
in the Cu/AAO-HWT catalysts can be explained by the increased surface area of hydrated supports and its effect on catalytic activity can be observed in the next section. The XRD profiles for the series of Cu/AAO catalysts and the support itself was shown in Fig. 3. The Cu/AAO-120 s and Cu/AAO-150 s catalysts shows strong peaks of Cu indicating the presence of bulk species on the surface and the Al and Al_2O_3 peaks are suppressed due to shielding of the AAO surface with Cu metal particles. The SEM analysis for AAO, AAO-HWT, Cu/AAO and Cu/AAO-HWT samples are shown in Figs. 4 and 5 which confirms the micropores formation on AAO surface and impregnation of Cu in the pores of alumina throughout the film. As shown in Fig 4(a), AAO formed with uniform pores at the optimum conditions of 24 h anodization in 0.3 M oxalic acid at 10 °C with a pore size of 50–60 nm. Similarly, SEM morphology of AAO-HWT can be seen which shows a change in surface as the Al_2O_3 structure is transformed to hydrated alumina. As shown in Fig. 5(a), a large number of small fragments were observed on the surface of AAO-HWT sample micrograph. Moreover, the fragment size was obviously decreased with increasing HWT time. Accordingly, the improved thermal stability may be obtained because of these smaller alumina fragments formation due to the HWT treatment, which are believed to absorb the expansion stress during heating and contraction stress during sudden cooling. Therefore these fragments may play the role of stress buffer in the expansion and contraction of the support. In addition, the enlarged surface area of the anodic alumina layer caused by the HWT treatment cannot be neglected, because it also acted as a stress buffer. The presence of Cu is revealed by EDX pattern as shown in Fig. 6. It is evident that the resulted nanoporous layer mainly consists of Cu metal particles.

3.2. Effect of Cu electrodeposition time on SRM conversion

Fig. 7 shows that the methanol conversion systematically increased with increasing temperature from 160 to 360 °C for all the tested catalysts. The dependence of conversion on temperature was remarkable for the Cu/AAO 120 s and Cu/AAO 150 s catalysts. Since at low reaction temperatures the activity is low for all the tested catalysts, that because of the steric effect may limit the rate of diffusion of the methanol molecules into the micropores of the catalyst and may also hinder the adsorption and reaction on the

Table 1
Characteristics of the various catalysts.

Catalyst	BET surface area ($m^2 g^{-1}$)	Copper metal surface area ($m^2 g^{-1}$)	Cu loading was obtained with ICP-OES (wt.%)
AAO as prepared	28.8	–	–
AAO-HWT-30 min	38.9	–	–
AAO-HWT-1 h	47.21	–	–
AAO-HWT-2 h	43.54	–	–
AAO-HWT-3 h	41.12	–	–
Cu/AAO-30 s	24.2	0.846	1.42
Cu/AAO-60 s	18.1	1.54	1.98
Cu/AAO-90 s	17.32	1.89	2.86
Cu/AAO-120 s	16.8	2.81	4.152
Cu/AAO-150 s	16.24	2.94	4.28
Cu/AAO-HWT 30 min	32.61	3.29	4.49
Cu/AAO-HWT 1 h	36.58	3.82	5.218
Cu/AAO-HWT 2 h	34.9	3.65	5.24
Cu/AAO-HWT 3 h	35.07	3.2	5.18

Fig. 3. XRD scan of Cu metal particles electrodeposited into an AAO template. Most visible are the Al peaks (●) from the substrate, Al_2O_3 peaks (△) and deposited Cu metal particle (<111>, <200>,<220>) peaks are indicated with (◆).
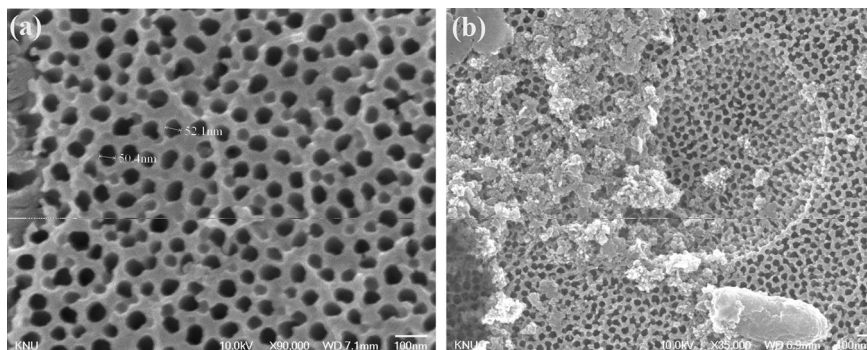
Fig. 4. The surface FE-SEM images of (a) AAO, and (b) Cu loaded AAO through electrodeposition.
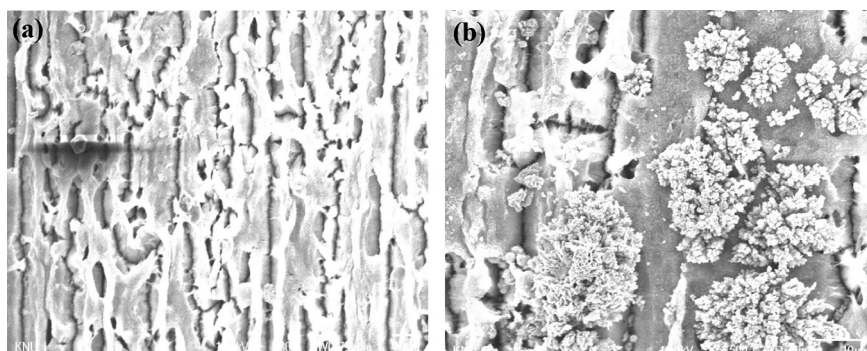

Fig. 5. The surface FE-SEM images of (a) AAO-HWT, and (b) Cu loaded AAO-HWT through electrodeposition.

active sites, which was diminished by the rapid movement of molecules due to a higher kinetic energy at high reaction temperatures. Hence, both the conversion and copper metal surface area (as shown in Table 1) with respect to copper loading had a similar trend. Consequently, we think that the SRM activity of the catalysts is dependent on the free exposed copper sites available for methanol molecule adsorption and reaction. When the copper electrodeposition time exceeds 120 s, the improvement in methanol conversion was negligible (for Cu/AAO 150 s catalyst) or may be low. The selectivity to CO_2 with respect to temperature was shown in Fig. 8, and it indicates that, for all the prepared Cu/AAO catalysts, the selectivity to CO_2 is less due to the formation of dimethyl ether (DME) especially at higher operating temperatures (320—360 °C) and the DME formation (Fig. 9) much higher for the catalysts prepared with low deposition time. The reason may be due to the surface acidic sites of γ-alumina and it may be responsible for the dimerization of methanol. When increasing the Cu electroplating time on AAO resulted in the formation of bulk copper on the surface with 120 s and 150 s deposition time and it leads to high CO_2 selectivity. Mainly the DME product was observed in the case of Cu/AAO 30 s, Cu/AAO 60 s and Cu/AAO 90 s in the temperature range of 300—360 °C and from 230 to 250 °C for Cu/AAO 120 s and Cu/AAO 150 s.

It was concluded that the AAO surface was fully saturated with Cu metal particles for deposition time $\geq$120 s and shields relatively more acid sites of alumina. In the case of lower deposition time the available AAO micropores were not sufficiently plated with copper metal particles and these acid sites could not contribute to the dehydration reaction.

3.3. Effect of hot water treatment on SRM conversion

The Cu/AAO-HWT series catalysts have high copper content and exhibited higher conversion and better CO_2 selectivity compared to

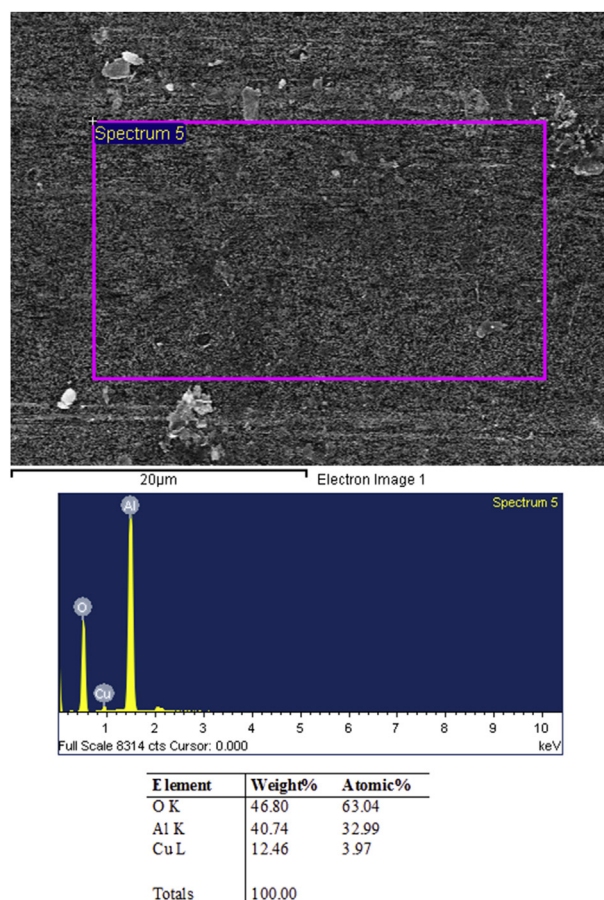| Element	Weight%	Atomic%
O K	46.80	63.04
Al K	40.74	32.99
Cu L	12.46	3.97
Totals	100.00	

Fig. 6. EDX analysis for Cu/AAO-120 s catalyst.
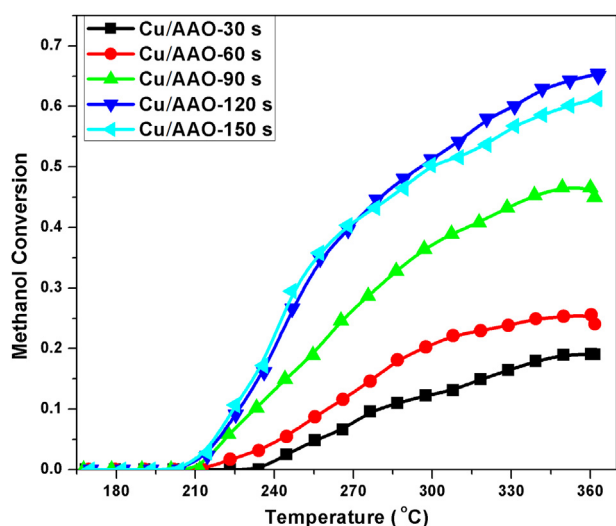
Fig. 7. Conversion of methanol over Cu/AAO catalysts, Cu electrodeposition time varied from 30 to 150 s.

Fig. 9. Effect of electrodeposition time on DME selectivity with temperature during SRM.

the Cu/AAO catalysts (for comparison methanol conversion and CO_2 selectivity for Cu/AAO-120 s catalyst was shown in Figs. 10 and 11), and it indicates that, the Cu/AAO-HWT catalysts showed a methanol conversion of 76, 86, 83 and 82% at 350 °C for Cu/AAO-HWT 30 min, Cu/AAO-HWT 1 h, Cu/AAO-HWT 2 h and Cu/AAO-HWT 3 h catalysts, respectively. Whereas, the Cu/AAO-120 s catalyst was shown only 64% of methanol conversion at the same reaction temperature. Selectivity to CO_2 for AAO-HWT series catalysts was shown in Fig. 11, and it was 100% for Cu/AAO-HWT 1 h, Cu/AAO-HWT 2 h and Cu/AAO-HWT 3 h catalysts in 200–350 °C temperature range and Cu/AAO-HWT 30 min catalyst was shown little less CO_2 selectivity in the 310–350 °C temperature range. The catalyst contained high copper content (Cu/AAO-HWT 1 h, Cu/AAO-HWT 2 h and Cu/AAO-HWT 3 h) has shown better CO_2 selectivity. The formation of DME with respect to temperature was shown in Fig. 12, the results were indicates that below 350 °C, DME formation was observed only in the case of Cu/AAO-HWT 30 min catalyst. Methanol conversion and CO_2 selectivity was less for Cu/AAO-120 s though the copper content was high (4.152 wt.%) which could be
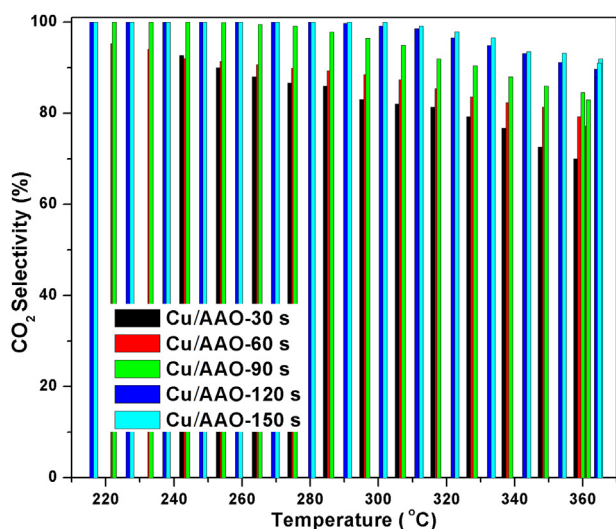
explained because of highly dispersed Cu in the pores of alumina. The reason behind the low activity of Cu/AAO series catalysts were may be due to the lower specific surface area of AAO support, which is much lesser than AAO-HWT support. As described in the experimental and characterization section, HWT treatment could produce a support with high surface area, at the same time the unfavorable sealing of pores would occur, because of the increased hydrated alumina sol in the pore skeleton and the expansion of the Al_2O_3 layer. This takes place especially at the top of the pores, where the reaction of Al_2O_3 with hot water is most rapid. Water diffusion into the micropores may inhibit due to the pores sealing, and eventually stop further hydration at the bottom of the pores. Therefore, as reported elsewhere [32], before HWT, PWT was conducted in an oxalic acid solution for 4 h at 30 °C to widen the pore radius and allow more alumina to react with hot water to form hydrated alumina, especially at the bottom of the pores. After the subsequent HWT and calcination, the surface area of the supports could be enlarged, as compared with samples without HWT. However, further HWT treatments caused a gradual decrease in
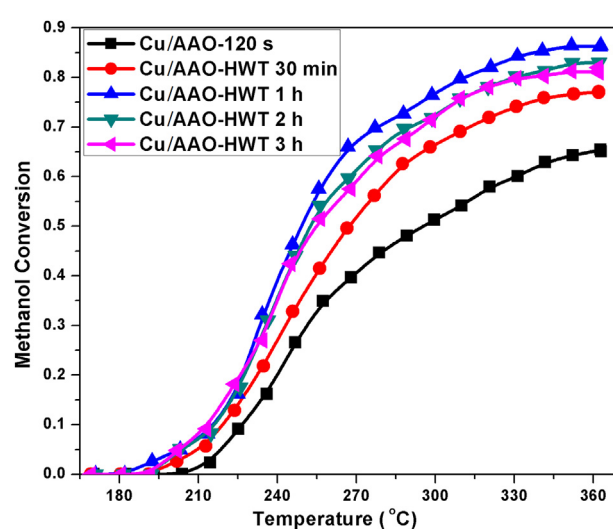

Fig. 8. Effect of electrodeposition time on CO_2 selectivity with temperature during SRM.

Fig. 10. Conversion of methanol over Cu/AAO-HWT catalysts, HWT treatment time varied from 30 min to 3 h.
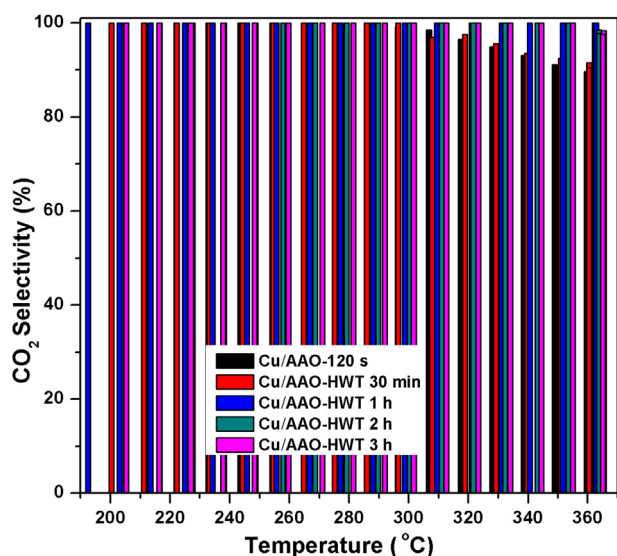
Fig. 11. Effect of HWT time on CO_2 selectivity with temperature in SRM reaction.

using a novel electrodeposition technique and the effects of electrodeposition time and HWT time of copper-plated AAOs on SRM conversion were investigated. The experimental data indicates that the Cu/AAO based catalysts prepared by electrodeposition method with respect to Cu-plating time showed promising methanol conversion results. In addition, methanol conversion and CO_2 selectivity was linearly increased with increasing copper content in the AAOs. Among the Cu/AAO catalysts Cu/AAO-120 s was shown 65% of methanol conversion at 350 °C with 91% selectivity towards CO_2 and the DME selectivity was 4.5%. It could be concluded that the copper content in AAOs played an important role in improving the methanol conversion and CO_2 selectivity, and the higher copper metal loading appeared to produce an increase in the characteristics of SRM conversion in spite of the decrease of specific surface area of the catalysts and increase in copper metal surface area. Further methanol conversion and CO_2 selectivity were improved over AAO-HWT supported catalysts and it was observed that the optimum HWT time was 1 h. The Cu/AAO-HWT 1 h gave a methanol conversion of about 86% at 350 °C, resulting in a CO_2 selectivity of 100%. These results indicate that the copper electroplating on AAOs is a useful technique for the SRM reaction with a viewpoint to highly functional metallic catalytic systems.

Acknowledgment

surface area, as shown in Table 1. Ganley et al. [33] also reported a similar phenomenon that after one hydrothermal-thermal treatment, the surface area of the anodic alumina increased from 2.5 to 25 $m^2 g^{-1}$. Correspondingly, as the number of treatments increased, the pore structure of the anodic alumina film fragmented. Yu Guo et al. [34] and Zhou et al. [24] also observed similar trend (decrease of surface area) when calcining the support in air or steam at 700 °C. In the present work also we observed similar phenomenon that the surface area of AAO-HWT 1 h was higher than AAO-HWT 2 h and AAO-HWT 3 h supports, hence it was shown better methanol conversion as well as higher selectivity towards CO_2.

4. Conclusions

Anodized aluminum oxide (AAO) templates with pore diameter range between 50 and 60 nm were synthesized using an oxalic acid based anodic oxidation process and the surface area of prepared AAO templates was enhanced by hot water treatment technique. Series of Cu/AAO and Cu/AAO-HWT catalysts were synthesized

Fig. 12. Effect of HWT time on DME selectivity with temperature in SRM reaction.

References

[1] S. Hocevar, W. Summers, in: A. Léon (Ed.), Hydrogen Technology, Springer, Berlin, 2008, pp. 15—79.
[2] X. Yan, S. Wang, X. Li, M. Hou, Z. Yuan, D. Li, L. Pan, C. Zhang, J. Liu, P. Ming, B. Yi, J. Power Sources 162 (2006) 1265—1269.
[3] S. Patel, K.K. Pant, J. Power Sources 159 (2006) 139—143.
[4] D.R. Sahoo, S. Vajpai, S. Patel, K.K. Pant, Chem. Eng. J. 125 (2007) 139—147.
[5] T.A. Semelsberger, K.C. Ott, R.L. Borup, H.L. Greene, Appl. Catal. A Gen. 309 (2006) 210—223.
[6] G. Busca, U. Costantino, F. Marmottini, T. Montanari, P. Patrono, F. Pinzari, G. Ramis, Appl. Catal. A Gen. 310 (2006) 70—78.
[7] H. Jeong, K.I. Kim, T.H. Kim, C.H. Ko, H.C. Park, I.K. Song, J. Power Sources 159 (2006) 1296—1299.
[8] S. Patel, K.K. Pant, J. Porous Mater. 13 (2006) 373—378.
[9] H. Yang, P. Liao, Appl. Catal. A Gen. 317 (2007) 226—233.
[10] J. Agrell, H. Birgersson, M. Boutonnet, I. Melian-Cabrera, R.M. Navarro, J.L.G. Fierro, J. Catal. 219 (2003) 389—403.
[11] H. Purnama, T. Ressler, R.E. Jentoft, H. Soerijanto, R. Schlogl, R. Schomacker, Appl. Catal. A Gen. 259 (2004) 83—94.
[12] N. Edwards, S.R. Ellis, J.C. Frost, S.E. Golunski, A.N.J. van Keulen, N.G. Lindewald, J.G. Reinkingh, J. Power Sources 71 (1998) 123—128.
[13] A. Karim, J. Bravo, D. Gorm, T. Conant, A. Datye, Catal. Today 110 (2005) 86—91.
[14] D.H. Kim, J. Lee, Stud. Surf. Sci. Catal. 159 (2006) 685—688.
[15] G.E. Jai Poinern, N. Ali, D. Fawcett, Materials 4 (2011) 487—526.
[16] B.Y. Yu, K.H. Lee, K. Kim, D.J. Byun, H.P. Ha, J.Y. Byun, J. Nanosci. Nanotechnol. 11 (2011) 6298—6305.
[17] T. Take, T. Yachi, M. Tomura, C. Kiyohara, T. Ishino, H. Kameyama, J. Chem. Eng. Jpn. 36 (2003) 271—276.
[18] T. Vergunst, F. Kapteijn, J.A. Moulijn, Appl. Catal. A Gen. 213 (2001) 179—187.
[19] B. Lindstrom, L.J. Pettersson, J. Power Sources 106 (2002) 264—273.
[20] E. Arendt, A. Maione, A. Klisinska, O. Sanz, M. Montes, S. Suarez, J. Blanco, P. Ruiz, Appl. Catal. A Gen. 339 (2008) 1—14.
[21] D.K. Liguras, K. Goundani, X.E. Verykios, J. Power Sources 130 (2004) 30—37.
[22] C. Fukuhara, K. Kawamorita, Appl. Catal. A Gen. 370 (2009) 42—49.
[23] Y. Guo, L. Zhou, H. Kameyama, Int. J. Hydrogen Energy 36 (2011) 5321—5333.
[24] L. Zhou, Y. Guo, M. Yagi, M. Sakurai, H. Kameyama, Int. J. Hydrogen Energy 34 (2009) 844—858.
[25] C. Fukuhara, H. Ohkura, Y. Kamata, Y. Murakami, A. Igarashi, Appl. Catal. A Gen. 273 (2004) 125—132.
[26] C. Fukuhara, H. Ohkura, K. Gonohe, A. Igarashi, Appl. Catal. A Gen. 279 (2005) 195—203.
[27] C. Fukuhara, Y. Kamata, A. Igarashi, Appl. Catal. A Gen. 296 (2005) 100—107.
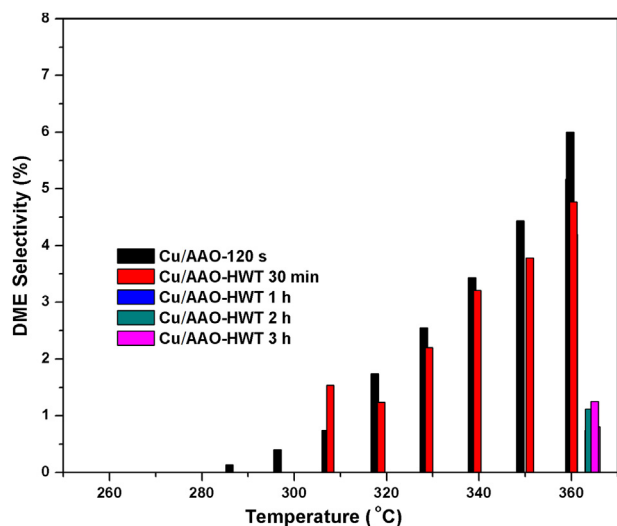[28] C. Fukuhara, Y. Kamata, A. Igarashi, Appl. Catal. A Gen. 330 (2007) 108—116.

[29] S.J. Park, B.J. Kim, J. Colloid Interface Sci. 292 (2005) 493–497.
[30] K. Nielsch, F. Muller, A.P. Li, U. Gosele, Adv. Mater. 12 (2000) 582–586.
[31] J.W. Evans, M.S. Wainwright, A.J. Bridgewater, D.J. Young, Appl. Catal. 7 (1983) 75–83.
[32] T.P. Tran, Y. Guo, J. Chen, L. Zhou, M. Sakurai, H. Kameyama, J. Chem. Eng. Jpn. 41 (2008) 1042–1048.
[33] J.C. Ganley, K.L. Riechmann, E.G. Seebauer, R.I. Masel, J. Catal. 227 (2004) 26–32.
[34] Y. Guo, L. Zhou, H. Kameyama, Chem. Eng. J. 168 (2011) 341–350.